

Lipschitz regularity of deep neural networks: analysis and efficient estimation

Kevin Scaman, Aladin Virmaux

Noah's Ark Lab, Huawei Technologies, Paris

{kevin.scaman, aladin.virmaux}@huawei.com

Abstract

Deep neural networks are notorious for being sensitive to small well-chosen perturbations, and estimating the regularity of such architectures is of utmost importance for safe and robust practical applications. In this paper, we investigate one of the key characteristics to assess the regularity of such methods: the Lipschitz constant of deep learning architectures. First, we show that, even for two layer neural networks, the exact computation of this quantity is NP-hard and state-of-art methods may significantly overestimate it. Then, we both extend and improve previous estimation methods by providing *AutoLip*, the first generic algorithm for upper bounding the Lipschitz constant of any automatically differentiable function. We provide a power method algorithm working with automatic differentiation, allowing efficient computations even on large convolutions. Second, for sequential neural networks, we propose an improved algorithm named *SeqLip* that takes advantage of the linear computation graph to split the computation per pair of consecutive layers. Third we propose heuristics on *SeqLip* in order to tackle very large networks. Our experiments show that *SeqLip* can significantly improve on the existing upper bounds.

1 Introduction

Deep neural networks made a striking entree in machine learning and quickly became state-of-the-art algorithms in many tasks such as computer vision [1, 2, 3, 4], speech recognition and generation [5, 6] or natural language processing [7, 8].

However, deep neural networks are known for being very sensitive to their input, and *adversarial examples* provide a good illustration of their lack of robustness [9, 10]. Indeed, a well-chosen small perturbation of the input image can mislead a neural network and significantly decrease its classification accuracy. One metric to assess the robustness of neural networks to small perturbations is the *Lipschitz constant* (see Definition 1), which upper bounds the relationship between input perturbation and output variation for a given distance. For generative models, the recent *Wasserstein GAN* [11] improved the training stability of GANs by reformulating the optimization problem as a minimization of the Wasserstein distance between the real and generated distributions [12]. However, this method relies on an efficient way of constraining the Lipschitz constant of the critic, which was only partially addressed in the original paper, and the object of several follow-up works [13, 14].

Recently, the Lipschitz continuity was used in order to improve the state-of-the-art in several deep

learning topics: (1) for robust learning, avoiding adversarial attacks was achieved in [15] by constraining local Lipschitz constants in neural networks. (2) For generative models, using spectral normalization on each layer allowed [13] to successfully train a GAN on ILRSVRC2012 dataset.

Our aim in this paper is to provide a rigorous and practice-oriented study on how Lipschitz constants of neural networks and automatically differentiable functions may be estimated. We first precisely define the notion of Lipschitz constant of vector valued functions in Section 2, and then show in Section 3 that its estimation is, even for 2-layer *Multi-Layer-Perceptrons* (MLP), NP-hard. In Section 4, we both extend and improve previous estimation methods by providing *AutoLip*, the first generic algorithm for upper bounding the Lipschitz constant of any automatically differentiable function. Moreover, we show how the Lipschitz constant of most neural network layers may be computed efficiently using automatic differentiation algorithms [16] and libraries such as PyTorch [17]. Notably, we extend the power method to convolution layers using automatic differentiation to speed-up the computations. In Section 6, we provide a theoretical analysis of *AutoLip* in the case of sequential neural networks, and show that the upper bound may lose a multiplicative factor *per activation layer*, which may significantly downgrade the estimation quality of *AutoLip* and lead to a very large and unrealistic upper bound. In order to prevent this, we propose an improved algorithm called *SeqLip* in the case of sequential neural networks, and show in Section 7 that *SeqLip* may significantly improve on *AutoLip*. Finally we discuss the different algorithms on the AlexNet [1] neural network for computer vision using the proposed algorithms.

2 Background and notations

In the following, we denote as $\langle x, y \rangle$ and $\|x\|_2$ the scalar product and L_2 -norm of the Hilbert space \mathbb{R}^n , $x \cdot y$ the coordinate-wise product of x and y , and $f \circ g$ the composition between the functions $f : \mathbb{R}^k \rightarrow \mathbb{R}^m$ and $g : \mathbb{R}^n \rightarrow \mathbb{R}^k$. For any differentiable function $f : \mathbb{R}^n \rightarrow \mathbb{R}^m$ and any point $x \in \mathbb{R}^n$, we will denote as $D_x f \in \mathbb{R}^{m \times n}$ the differential operator of f at x , also called the *Jacobian matrix*. Note that, in the case of real valued functions (i.e. $m = 1$), the gradient of f is the transpose of the differential operator: $\nabla f(x) = (D_x f)^\top$. Finally, $\text{diag}_{n,m}(x) \in \mathbb{R}^{n \times m}$ is the rectangular matrix with $x \in \mathbb{R}^{\min\{n,m\}}$ along the diagonal and 0 outside of it. When unambiguous, we will use the notation $\text{diag}(x)$ instead of $\text{diag}_{n,m}(x)$. All proofs are available in the appendix.

Definition 1. A function $f : \mathbb{R}^n \rightarrow \mathbb{R}^m$ is called *Lipschitz continuous* if there exists a constant L such that

$$\forall x, y \in \mathbb{R}^n, \|f(x) - f(y)\|_2 \leq L \|x - y\|_2.$$

The smallest L for which the previous inequality is true is called the *Lipschitz constant* of f and will be denoted $L(f)$.

For locally Lipschitz functions (i.e. functions whose restriction to some neighborhood around any point is Lipschitz), the Lipschitz constant may be computed using its differential operator.

Theorem 1 (Rademacher [18, Theorem 3.1.6]). *If $f : \mathbb{R}^n \rightarrow \mathbb{R}^m$ is a locally Lipschitz continuous function, then f is differentiable almost everywhere. Moreover, if f is Lipschitz continuous, then*

$$L(f) = \sup_{x \in \mathbb{R}^n} \|D_x f\|_2 \quad (1)$$

where $\|M\|_2 = \sup_{\{x : \|x\|=1\}} \|Mx\|_2$ is the operator norm of the matrix $M \in \mathbb{R}^{m \times n}$.

In particular, if f is real valued (i.e. $m = 1$), its Lipschitz constant is the maximum norm of its gradient $L(f) = \sup_x \|\nabla f(x)\|_2$ on its domain set. Note that the supremum in Theorem 1 is a slight abuse of notations, since the differential $D_x f$ is defined *almost everywhere* in \mathbb{R}^n , except for a set of Lebesgue measure zero.

3 Exact Lipschitz computation is NP-hard

In this section, we show that the exact computation of the Lipschitz constant of neural networks is **NP**-hard, hence motivating the need for good approximation algorithms. More precisely, upper bounds are in this case more valuable as they ensure that the variation of the function, when subject to an input perturbation, remains small. A *neural network* is, in essence, a succession of linear operators and non-linear activation functions. The most simplistic model of neural network is the *Multi-Layer-Perceptron* (MLP) as defined below.

Definition 2 (MLP). A K -layer *Multi-Layer-Perceptron* $f_{MLP} : \mathbb{R}^n \rightarrow \mathbb{R}^m$ is the function

$$f_{MLP}(x) = T_K \circ \rho_{K-1} \circ \cdots \circ \rho_1 \circ T_1(x),$$

where $T_k : x \mapsto M_k x + b_k$ is an affine function and $\rho_k : x \mapsto (g_k(x_i))_{i \in \llbracket 1, n_k \rrbracket}$ is a non-linear activation function.

Many standard deep network architectures (e.g. CNNs) follow –to some extent– the MLP structure. It turns out that even for 2-layer MLPs, the computation of the Lipschitz constant is **NP**-hard.

Problem 1 (LIP-CST). **LIP-CST** is the decision problem associated to the exact computation of the Lipschitz constant of a 2-layer MLP with ReLU activation layers.

Input: Two matrices $M_1 \in \mathbb{R}^{l \times n}$ and $M_2 \in \mathbb{R}^{m \times l}$, and a constant $\ell \geq 0$.

Question: Let $f = M_2 \circ \rho \circ M_1$ where $\rho(x) = \max\{0, x\}$ is the ReLU activation function. Is the Lipschitz constant $L(f) \leq \ell$?

Theorem 2 shows that, even for extremely simple neural networks, exact Lipschitz computation is not achievable in polynomial time (assuming that $\mathbf{P} \neq \mathbf{NP}$). The proof of Theorem 2 is available in Appendix A.

Theorem 2. *Problem 1 is NP-hard.*

Theorem 2 relies on a reduction to the **NP**-hard problem of quadratic concave minimization on a hypercube by considering well-chosen matrices M_1 and M_2 .

4 AutoLip: a Lipschitz upper bound through automatic differentiation

Efficient implementations of backpropagation in modern deep learning libraries such as *PyTorch* [17] or *TensorFlow* [19] rely on the concept of *automatic differentiation* [20, 16]. Simply put, automatic differentiation is a principled approach to the computation of gradients and differential operators of functions resulting from K successive operations.

Algorithm 1 AutoLip

Input: function $f : \mathbb{R}^n \rightarrow \mathbb{R}^m$ and its computation graph (g_1, \dots, g_K)

Output: upper bound on the Lipschitz constant: $\hat{L}_{AL} \geq L(f)$

1: $\mathcal{Z} = \{(z_0, \dots, z_K) : \forall k \in \llbracket 0, K \rrbracket, \theta_k \text{ is constant} \Rightarrow z_k = \theta_k(0)\}$

2: $L_0 \leftarrow 1$

3: **for** $k = 1$ to K **do**

4: $L_k \leftarrow \sum_{i=1}^{k-1} \max_{z \in \mathcal{Z}} \|\partial_i g_k(z)\|_2 L_i$

5: **end for**

6: **return** $\hat{L}_{AL} = L_k$

Definition 3. A function $f : \mathbb{R}^n \rightarrow \mathbb{R}^m$ is *computable in K operations* if it is the result of K simple functions in the following way: $\exists(\theta_1, \dots, \theta_K)$ functions of the input x and (g_1, \dots, g_K) where g_l is a function of $(\theta_i)_{i \leq l-1}$ such that:

$$\theta_0(x) = x, \quad \theta_K(x) = f(x), \quad \forall k \in \llbracket 1, K \rrbracket, \quad \theta_k(x) = g_k(x, \theta_1(x), \dots, \theta_{k-1}(x)). \quad (2)$$

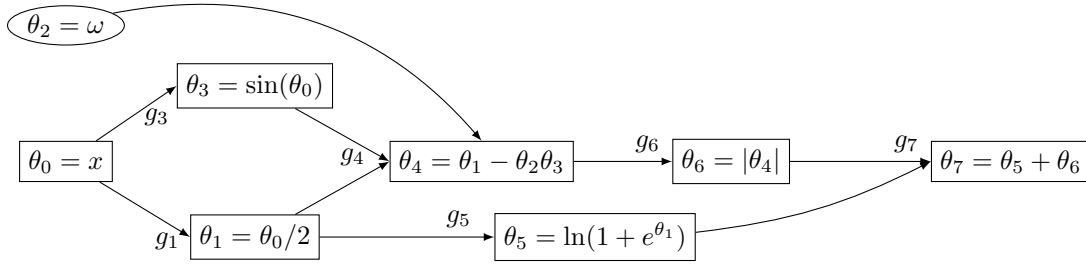


Figure 1: Example of a computation graph for $f_\omega(x) = \ln(1 + e^{x/2}) + |x/2 - \omega \sin(x)|$.

We assume that these operations are all locally Lipschitz-continuous, and that their partial derivatives $\partial_i g_k(x)$ can be computed and efficiently maximized. This assumption is discussed in Section 5 for the main operations used in neural networks. When the function is real valued (i.e. $m = 1$), the backpropagation algorithm allows to compute its gradient efficiently in time proportional to the number of operations K [21]. For the computation of the Lipschitz constant $L(f)$, a forward propagation through the computation graph is sufficient. More specifically, the chain rule immediately implies

$$D_x \theta_k = \sum_{i=1}^{k-1} \partial_i g_k(\theta_0(x), \dots, \theta_{k-1}(x)) D_x \theta_i, \quad (3)$$

and taking the norm then maximizing over all possible values of $\theta_i(x)$ leads to the *AutoLip* algorithm described in Alg. (1). This algorithm is an extension of the well known product of operator norms for MLPs (see e.g. [13]) to any function computable in K operations.

Proposition 1. For any MLP (see Definition 2) with 1-Lipschitz activation functions (e.g. ReLU,

Leaky ReLU, SoftPlus, Tanh, Sigmoid, ArcTan or Softsign), the AutoLip upper bound becomes

$$\hat{L}_{AL} = \prod_{k=1}^K \|M_k\|_2.$$

Note that, when the intermediate function θ_k does not depend on x , it is not necessary to take a maximum over all possible values of $\theta_k(x)$. To this end we define the set of feasible intermediate values as

$$\mathcal{Z} = \{(z_0, \dots, z_K) : \forall k \in \llbracket 0, K \rrbracket, \theta_k \text{ is constant} \Rightarrow z_k = \theta_k(0)\}, \quad (4)$$

and only maximize partial derivatives over this set. In practice, this is equivalent to removing branches of the computation graph that are not reachable from node 0 and replacing them by constant values. To illustrate this definition, consider a simple matrix product operation $f(x) = Wx$. One possible computation graph for f is $\theta_0 = x$, $\theta_1 = W$ and $\theta_2 = g_2(\theta_0, \theta_1) = \theta_1\theta_0$. While the quadratic function g_2 is not Lipschitz-continuous, its derivative w.r.t. θ_0 is bounded by $\partial_0 g_2(\theta_0, \theta_1) = \theta_1 = W$. Since θ_1 is constant relatively to x , we have $\mathcal{Z} = \{(x, 0)\}$ and the algorithm returns the exact Lipschitz constant $\hat{L}_{AL} = L(f) = \|W\|_2$.

Example. We consider the graph explicited on Figure 1. Since θ_2 is a constant w.r.t. x , we can replace it by its value ω in all other nodes. Then, the AutoLip algorithm runs as follows:

$$\hat{L}_{AL} = L_7 = L_6 + L_5 = L_1 + L_4 = 2L_1 + wL_3 = 1 + \omega. \quad (5)$$

Note that, in this example, the Lipschitz upper bound \hat{L}_{AL} matches the exact Lipschitz constant $L(f_\omega) = 1 + \omega$.

5 Lipschitz constants of typical neural network layers

Linear and convolution layers. The Lipschitz constant of an affine function $f : x \mapsto Mx + b$ where $M \in \mathbb{R}^{m \times n}$ and $b \in \mathbb{R}^m$ is the largest singular value of its associated matrix M , which may be computed efficiently, up to a given precision, using the *power method* [22]. In the case of convolutions, the associated matrix may be difficult to access and high dimensional, hence making the direct use of the power method impractical. To circumvent this difficulty, we extend the power method to any affine function on whose automatic differentiation can be used (e.g. linear or convolution layers of neural networks) by noting that the only matrix multiplication of the power method $M^\top Mx$ can be computed by differentiating a well-chosen function.

Lemma 1. *Let $M \in \mathbb{R}^{m \times n}$, $b \in \mathbb{R}^m$ and $f : x \mapsto Mx + b$ be an affine function. Then, for all $x \in \mathbb{R}^n$, we have*

$$M^\top Mx = \nabla g(x),$$

where $g(x) = \frac{1}{2}\|f(x) - f(0)\|_2^2$.

Proof. By definition, $g(x) = \frac{1}{2}\|Mx\|_2^2$, and differentiating this equation leads to the desired result. \square

Algorithm 2 AutoGrad compliant power method

Input: affine function $f : \mathbb{R}^n \rightarrow \mathbb{R}^m$, number of iteration N

Output: approximation of the Lipschitz constant $L(f)$

```
1: for  $k = 1$  to  $N$  do  
2:    $v \leftarrow \nabla g(v)$  where  $g(x) = \frac{1}{2} \|f(x) - f(0)\|_2^2$   
3:    $\lambda \leftarrow \|v\|_2$   
4:    $v \leftarrow v/\lambda$   
5: end for  
6: return  $L(f) = \|f(v) - f(0)\|_2$ 
```

The full algorithm is described in Alg. (2). Note that this algorithm is fully compliant with any dynamic graph deep learning libraries such as PyTorch. The gradient of the square norm may be computed through autograd, and the gradient of $L(f)$ may be computed the same way without any more programming effort. Note that the gradients w.r.t. M may also be computed with the closed form formula $\nabla_M \sigma = u_1 v_1^\top$ where u_1 and v_1 are respectively the left and right singular vector of M associated to the singular value σ [23]. The same algorithm may be straightforwardly iterated to compute the k -largest singular values.

Activation layers. An activation layer $\rho : \mathbb{R}^n \rightarrow \mathbb{R}^n$ applies a non-linear function $g : \mathbb{R} \rightarrow \mathbb{R}$ to every coordinate of the input vector

$$\rho(x) = (g(x_i))_{i \in \llbracket 1, n \rrbracket}, \quad (6)$$

and, using Theorem 1, its Lipschitz constant is simply the Lipschitz constant of g :

$$L(\rho) = \sup_{x \in \mathbb{R}^n} \|D_x \rho\|_2 = \sup_{x \in \mathbb{R}^n} \|\text{diag}(g'(x_i)_{i \in \llbracket 1, n \rrbracket})\|_2 = \sup_{x \in \mathbb{R}} |g'(x)| = L(g), \quad (7)$$

where the sup is taken almost everywhere.

When we apply a different activation function $g_i : \mathbb{R} \rightarrow \mathbb{R}$ to each coordinate $i \in \llbracket 1, n \rrbracket$, then the same calculation leads to $L(\rho) = \max_{i \in \llbracket 1, n \rrbracket} L(g_i)$. All main activation functions such as ReLU, Leaky ReLU, SoftPlus, Tanh, Sigmoid, ArcTan or Softsign have a Lipschitz constant equal to 1.

Dropout. At evaluation time, dropout [24] applies a factor p to the output vector to compensate for the coefficients randomly set to 0 during training, hence is an operator with Lipschitz constant p .

Batch Normalization. Batch Normalization [25] tracks running statistics over the different batches and uses these statistics at evaluation. It is a linear operator with parameters including the weights $(\gamma_i)_i$ and the running variance $(r_i)_i$. As a linear operator, Alg. (2) can be used to compute its Lipschitz constant. However, a simple closed-form solution is also available as

$$\max_i \left\{ \frac{\gamma_i}{\sqrt{r_i + \epsilon}} \right\}. \quad (8)$$

Pooling layers. A pooling layer reduces the dimensionality of the input vector using a non-linear function, for example by subsampling the coordinates of the input vector. *Maxpooling* has a Lipschitz constant equal to 1. *Average pooling* is a linear operation and hence can be computed with Alg. (2) and autograd. However, with a kernel of size k^d , its Lipschitz constant is $k^{-d/2}$ for the $\|\cdot\|_2$ norm.

6 Sequential neural networks

Despite its generality, AutoLip may be subject to large errors due to the multiplication of smaller errors at each iteration of the algorithm. In this section, we improve on the AutoLip upper bound by a more refined analysis of deep learning architectures in the case of MLPs. More specifically, the Lipschitz constant of MLPs have an explicit formula using Theorem 1 and the chain rule:

$$L(f_{MLP}) = \sup_{x \in \mathbb{R}^n} \|M_K \text{diag}(g'_{K-1}(\theta_{K-1})) M_{k-1} \dots M_2 \text{diag}(g'_1(\theta_1)) M_1\|_2, \quad (9)$$

where $\theta_k = T_k \circ \rho_{k-1} \circ \dots \circ \rho_1 \circ T_1(x)$ is the intermediate output after k linear layers.

Considering Proposition 1 and Eq. (9), the equality $\hat{L}_{AL} = L(f_{MLP})$ only takes place if all activation layers $\text{diag}(g'_k(\theta_k))$ map the first singular vector of M_k to the first singular vector of M_{k+1} by Cauchy-Schwarz inequality. However, differential operators of activation layers, being diagonal matrices, can only have a limited effect on input vectors, and in practice, first singular vectors will tend to misalign, leading to a drop in the Lipschitz constant of the MLP. This is the intuition behind *SeqLip*, an improved algorithm for Lipschitz constant estimation for MLPs.

6.1 SeqLip, an improved algorithm for MLPs

In Eq. (9), the diagonal matrices $\text{diag}(g'_{K-1}(\theta_{K-1}))$ are difficult to evaluate, as they may depend on the input value x and previous layers. Fortunately, as stated in Section 5, most major activation functions are 1-Lipschitz. More specifically, these activation functions have a derivative $g'_k(x) \in [0, 1]$. Hence, we may replace the supremum on the input vector x by a supremum over all possible values:

$$L(f_{MLP}) \leq \max_{\forall i, \sigma_i \in [0,1]^{n_i}} \|M_K \text{diag}(\sigma_{K-1}) \dots \text{diag}(\sigma_1) M_1\|_2, \quad (10)$$

where σ_i corresponds to all possible derivatives of the activation gate. Solving the right hand side of Eq. (10) is still a hard problem, and the high dimensionality of the search space $\sigma \in [0, 1]^{\sum_{i=1}^K n_i}$ makes purely combinatorial approaches prohibitive even for small neural networks. In order to decrease the complexity of the problem, we split the operator norm in $K - 1$ parts using the SVD decomposition of each matrix $M_i^\top = U_i \Sigma_i V_i^\top$ and the submultiplicativity of the operator norm:

$$\begin{aligned} L(f_{MLP}) &\leq \max_{\forall i, \sigma_i \in [0,1]^{n_i}} \|\Sigma_1 U_1^\top \text{diag}(\sigma_2) \Sigma_2 V_2 \text{diag}(\sigma_2) U_2^\top \Sigma_3 \dots \Sigma_{k-1} V_k \text{diag}(\sigma_k) \Sigma_k\|_2, \\ &\leq \prod_{i=1}^{k-1} \max_{\sigma_i \in [0,1]^{n_i}} \left\| \tilde{\Sigma}_i V_i \text{diag}(\sigma_i) U_{i+1}^\top \tilde{\Sigma}_{i+1} \right\|_2, \end{aligned} \quad (11)$$

where $\tilde{\Sigma}_i = \Sigma_i$ if $i \in \{1, k\}$ and $\tilde{\Sigma}_i = \Sigma_i^{1/2}$ otherwise. Each activation layer can now be solved independently, leading to the *SeqLip* upper bound:

$$\hat{L}_{SL} = \prod_{i=1}^{k-1} \max_{\sigma_i \in [0,1]^{n_i}} \left\| \tilde{\Sigma}_i V_i \text{diag}(\sigma_i) U_{i+1}^\top \tilde{\Sigma}_{i+1} \right\|_2. \quad (12)$$

When the inner layers are small ($n_i \leq 20$), a brute force combinatorial approach returns the result. Otherwise, we approximately solve each problem using a greedy heuristic: we first set $\sigma = 1$ and then perform a coordinate ascent until convergence to a local maximum. We call *Greedy SeqLip* this heuristic. In all our experiments on which the exact optimum is explicitly computable, the incurred error is less than 1%. Finally, when the dimension of the layer is too large to compute a whole SVD, we approximate it using the first singular values of the matrices M_i .

6.2 Theoretical analysis of SeqLip

In order to better understand how SeqLip may improve on AutoLip, we now consider a simple setting in which all linear layers have a large difference between their first and second singular values. For simplicity, we also assume that activation functions have a derivative $g'_k(x) \in [0, 1]$, although the following results easily generalize as long as the derivative remains bounded. Then, the following theorem holds.

Theorem 3. *Let M_k be the matrix associated to the k -th linear layer, u_k (resp. v_k) its first left (resp. right) singular vector, and $r_k = s_{k,2}/s_{k,1}$ the ratio between its second and first singular values. Then, we have*

$$\hat{L}_{SL} \leq \hat{L}_{AL} \prod_{k=1}^{K-1} \sqrt{(1 - r_k - r_{k+1}) \max_{\sigma \in [0,1]^{n_k}} \langle \sigma \cdot u_k, v_{k+1} \rangle^2 + r_k + r_{k+1} + r_k r_{k+1}}.$$

Note that $\max_{\sigma \in [0,1]^{n_k}} \langle \sigma \cdot u_k, v_{k+1} \rangle^2 \leq 1$ and, when the ratios r_k are negligible, then

$$\hat{L}_{SL} \leq \hat{L}_{AL} \prod_{k=1}^{K-1} \max_{\sigma \in [0,1]^{n_k}} |\langle \sigma \cdot u_k, v_{k+1} \rangle|. \quad (13)$$

Intuitively, each activation layer may align u_k to v_{k+1} only to a certain extent. Moreover, when the two singular vectors u_k and v_{k+1} are not too similar, this quantity can be substantially smaller than 1. To illustrate this idea, we now show that $\max_{\sigma \in [0,1]^{n_k}} |\langle \sigma \cdot u_k, v_{k+1} \rangle|$ is of the order of $1/\pi$ if the two vectors are randomly chosen on the unit sphere.

Lemma 2. *Let $x \geq 0$ and $u, v \in \mathbb{R}^n$ be two independent random vectors taken uniformly on the unit sphere $\mathbb{S}^{n-1} = \{x \in \mathbb{R}^n : \|x\|_2 = 1\}$. Then we have*

$$\max_{\sigma \in [0,1]^n} |\langle \sigma \cdot u, v \rangle| \xrightarrow{n \rightarrow +\infty} \frac{1}{\pi} \quad \text{almost surely.}$$

Intuitively, when the ratios between the second and first singular values are sufficiently small, each activation layer decreases the Lipschitz constant by a factor $1/\pi$ and

$$\hat{L}_{SL} \approx \frac{\hat{L}_{AL}}{\pi^{K-1}}. \quad (14)$$

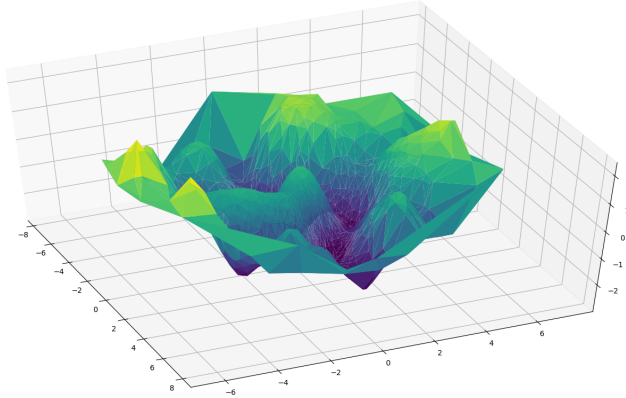


Figure 2: Synthetic function used to train a 5-layer MLP

For example, for $K = 5$ linear layers, we have $\pi^{K-1} \approx 100$ and a large improvement may be expected for SeqLip compared to AutoLip. Of course, in a more realistic setting, the eigenvectors of different layers are not independent and, more importantly, the ratio between second and first eigenvalues may not be sufficiently small. However, this simple setting provides us with the best improvement one can hope for, and our experiments in Section 7 shows that at least part of the suboptimality of AutoLip is due to the misalignment of eigenvectors.

7 Experimentations

As stated in Theorem 2 computing the Lipschitz constant is an **NP**-hard problem. However, in low dimension (e.g. $d \leq 5$), optimizing the problem in Eq. (1) can be performed efficiently using a simple grid search. This will provide a baseline to compare the different estimation algorithms. In high dimension, grid search is intractable and we consider several other estimation methods: (1) random search for Eq. (1), (2) simulated annealing for Eq. (1), (3) product of Frobenius norms of linear layers [13], (4) product of spectral norms [13] (equivalent to AutoLip in the case of MLPs). Note that, for MLPs with ReLU activations, first order optimization methods such as SGD are inefficient because the function to optimize in Eq. (1) is piecewise constant. The method (1), (2) gives a lower bound and (3), (4) gives an upper bound on the Lipschitz constant.

MLP. We construct a 2-dimensional dataset from a Gaussian Process with RBF Kernel with mean 0 and variance 1. We use 2000 generated points as a synthetic dataset. An example of such a dataset may be seen in Figure 2.

We train a 5-layer MLP with 20 neurons at each layer on the synthetic dataset with MSE loss and ReLU activations. Note that in this particular simulation, the greedy SeqLip algorithm gives the same upper-bound as SeqLip, which justify its usage in high dimension.

Lower bounds		Upper bounds		Approximation of upper bound	
Grid search	5.3	Frobenius Norm	4240	Greedy SeqLip	59.7
Annealing	2.9	AutoLip	253		
		SeqLip	59.7		

First, since the dimension is low ($d = 2$), grid search returns a very good approximation of the Lipschitz constant, while simulated annealing is suboptimal, probably due to the presence of local maxima. For upper bounds, SeqLip outperforms its competitors and improves on AutoLip by a factor of 4, reducing the gap between upper bounds and, in this case, the true Lipschitz constant computed using grid search.

CNN. We train a very simple 4-layers CNN classifier on the MNIST dataset [26] with 99.14% accuracy on the test set. The structure of the CNN is described in Appendix D.

Lower bound		Upper bound		Approximation of upper bound	
Annealing	25.5	Spectral	174	Greedy SeqLip (200 singular values)	86

SeqLip improves by a factor of 2 the upper bound given by AutoLip. Note that the lower bound obtained with simulated annealing is probably too low, as shown in the previous experiment, and the true Lipschitz constant probably lies in the interval $[25, 86]$.

AlexNet. AlexNet [1] is one of the first success of deep learning in computer vision. The AutoLip algorithm finds that the Lipschitz constant is upper bounded by 3.62×10^7 which remains extremely large and probably well above the true Lipschitz constant. As for the experiment on a CNN, we use the 200 highest singular values of each linear layer for computing Greedy SeqLip. We obtain 5.45×10^6 as approximation of the upper bound, which remains very large despite its 6 fold improvement over AutoLip.

8 Conclusion

In this paper, we studied the Lipschitz regularity of neural networks. We first showed that the exact computation of the Lipschitz constant is an **NP**-hard problem. We then provided a generic upper bound called *AutoLip* for the Lipschitz constant of any automatically differentiable function. In doing so, we introduced an algorithm to compute singular values of affine operators such as convolution in a very efficient way using *autograd* mechanism. We finally proposed a refinement of the previous methods called *SeqLip* for MLPs and showed how this algorithm can improve on AutoLip theoretically and in applications, sometimes improving up to a factor of 10 the AutoLip upper bound.

Acknowledgements

The authors thank the whole team at Huawei Paris and in particular Igor Colin, Moez Draief, Sylvain Robbiano and Albert Thomas for useful discussions and feedback.

References

- [1] Alex Krizhevsky, Ilya Sutskever, and Geoffrey E Hinton. Imagenet classification with deep convolutional neural networks. In *Advances in Neural Information Processing Systems*, pages 1097–1105, 2012.
- [2] Christian Szegedy, Vincent Vanhoucke, Sergey Ioffe, Jon Shlens, and Zbigniew Wojna. Rethinking the inception architecture for computer vision. In *Proceedings of the IEEE Conference on Computer Vision and Pattern Recognition (CVPR)*, pages 2818–2826, 2016.
- [3] Kaiming He, Xiangyu Zhang, Shaoqing Ren, and Jian Sun. Deep residual learning for image recognition. In *Proceedings of the IEEE Conference on Computer Vision and Pattern Recognition (CVPR)*, pages 770–778, 2016.
- [4] G. Huang, Z. Liu, L. v. d. Maaten, and K. Q. Weinberger. Densely connected convolutional networks. In *Proceedings of the IEEE Conference on Computer Vision and Pattern Recognition (CVPR)*, pages 2261–2269, 2017.
- [5] Alex Graves and Navdeep Jaitly. Towards end-to-end speech recognition with recurrent neural networks. In *International Conference on Machine Learning*, pages 1764–1772, 2014.
- [6] Aäron van den Oord, Sander Dieleman, Heiga Zen, Karen Simonyan, Oriol Vinyals, Alex Graves, Nal Kalchbrenner, Andrew W. Senior, and Koray Kavukcuoglu. Wavenet: A generative model for raw audio. In *SSW*, page 125. ISCA, 2016.
- [7] Tomas Mikolov, Wen-tau Yih, and Geoffrey Zweig. Linguistic regularities in continuous space word representations. In *Proceedings of the 2013 Conference of the North American Chapter of the Association for Computational Linguistics: Human Language Technologies*, pages 746–751, 2013.
- [8] Ashish Vaswani, Noam Shazeer, Niki Parmar, Jakob Uszkoreit, Llion Jones, Aidan N Gomez, Łukasz Kaiser, and Illia Polosukhin. Attention is All You Need. In *Advances in Neural Information Processing Systems*, pages 6000–6010, 2017.
- [9] Christian Szegedy, Wojciech Zaremba, Ilya Sutskever, Joan Bruna, Dumitru Erhan, Ian Goodfellow, and Rob Fergus. Intriguing properties of neural networks. In *Proceedings of the International Conference on Learning Representations (ICLR)*, 2014.
- [10] Ian J Goodfellow, Jonathon Shlens, and Christian Szegedy. Explaining and harnessing adversarial examples. In *Proceedings of the International Conference on Learning Representations (ICLR)*, 2015.
- [11] Martín Arjovsky, Soumith Chintala, and Léon Bottou. Wasserstein generative adversarial networks. In *Proceedings of the 34th International Conference on Machine Learning, ICML*, pages 214–223, 2017.
- [12] Cédric Villani. *Optimal transport: old and new*, volume 338. Springer Science & Business Media, 2008.
- [13] Takeru Miyato, Toshiki Kataoka, Masanori Koyama, and Yuichi Yoshida. Spectral normalization for generative adversarial networks. In *Proceedings of the International Conference on Learning Representations (ICLR)*, 2018.

- [14] Ishaan Gulrajani, Faruk Ahmed, Martin Arjovsky, Vincent Dumoulin, and Aaron C Courville. Improved training of Wasserstein GANs. In *Advances in Neural Information Processing Systems*, pages 5769–5779, 2017.
- [15] Tsui-Wei Weng, Huan Zhang, Pin-Yu Chen, Jinfeng Yi, Dong Su, Yupeng Gao, Cho-Jui Hsieh, and Luca Daniel. Evaluating the Robustness of Neural Networks: An Extreme Value Theory Approach. In *Proceedings of the International Conference on Learning Representations (ICLR)*, 2018.
- [16] Louis B. Rall. *Automatic Differentiation: Techniques and Applications*, volume 120 of *Lecture Notes in Computer Science*. Springer, Berlin, 1981.
- [17] Adam Paszke, Sam Gross, Soumith Chintala, Gregory Chanan, Edward Yang, Zachary DeVito, Zeming Lin, Alban Desmaison, Luca Antiga, and Adam Lerer. Automatic differentiation in PyTorch. 2017.
- [18] Herbert Federer. *Geometric measure theory*. Classics in Mathematics. Springer-Verlag Berlin Heidelberg, 1969.
- [19] Martín Abadi, Ashish Agarwal, Paul Barham, Eugene Brevdo, Zhifeng Chen, Craig Citro, Greg S. Corrado, Andy Davis, Jeffrey Dean, Matthieu Devin, Sanjay Ghemawat, Ian Goodfellow, Andrew Harp, Geoffrey Irving, Michael Isard, Yangqing Jia, Rafal Jozefowicz, Lukasz Kaiser, Manjunath Kudlur, Josh Levenberg, Dandelion Mané, Rajat Monga, Sherry Moore, Derek Murray, Chris Olah, Mike Schuster, Jonathon Shlens, Benoit Steiner, Ilya Sutskever, Kunal Talwar, Paul Tucker, Vincent Vanhoucke, Vijay Vasudevan, Fernanda Viégas, Oriol Vinyals, Pete Warden, Martin Wattenberg, Martin Wicke, Yuan Yu, and Xiaoqiang Zheng. TensorFlow: Large-Scale Machine Learning on Heterogeneous Systems, 2015. Software available from tensorflow.org.
- [20] Andreas Griewank and Andrea Walther. *Evaluating derivatives: principles and techniques of algorithmic differentiation*, volume 105. Siam, 2008.
- [21] Seppo Linnainmaa. The representation of the cumulative rounding error of an algorithm as a Taylor expansion of the local rounding errors. *Master’s Thesis (in Finnish), Univ. Helsinki*, pages 6–7, 1970.
- [22] RV Mises and Hilda Pollaczek-Geiringer. Praktische verfahren der gleichungsauflösung. *ZAMM-Journal of Applied Mathematics and Mechanics/Zeitschrift für Angewandte Mathematik und Mechanik*, 9(1):58–77, 1929.
- [23] Jan R. Magnus. On Differentiating Eigenvalues and Eigenvectors. *Econometric Theory*, 1(2):pp. 179–191, 1985.
- [24] Nitish Srivastava, Geoffrey Hinton, Alex Krizhevsky, Ilya Sutskever, and Ruslan Salakhutdinov. Dropout: A simple way to prevent neural networks from overfitting. *The Journal of Machine Learning Research*, 15(1):1929–1958, 2014.
- [25] Sergey Ioffe and Christian Szegedy. Batch normalization: Accelerating deep network training by reducing internal covariate shift. In *Proceedings of the 32nd International Conference on Machine Learning, ICML*, pages 448–456, 2015.
- [26] Yann LeCun. The MNIST database of handwritten digits. <http://yann.lecun.com/exdb/mnist/>.

[27] Reiner Horst and Panos M Pardalos. *Handbook of global optimization*, volume 2. Springer Science & Business Media, 2013.

A Proof of Theorem 2

We reduce the problem of maximizing a quadratic convex function on a hypercube to **LIP-CST**. Start from the following NP-hard problem [27, Quadratic Optimization, Section 4]:

$$\begin{aligned} & \underset{\sigma}{\text{maximize}} && \sum_i (h_i^\top \sigma)^2 = \sigma^\top H \sigma \\ & \text{s. t.} && \forall k, 0 \leq \sigma_k \leq 1, \end{aligned} \quad (15)$$

where $H = \sum_i h_i h_i^\top$ is a positive semi-definite matrix with full rank. Let's note

$$M_1 = \left(\begin{array}{c|c|c|c} h_1 & h_2 & \cdots & h_n \end{array} \right), \quad M_2 = \left(\begin{array}{c|c} 1 & \\ \vdots & \\ 1 & 0 \end{array} \right)$$

so that we have

$$M_2 \text{diag}(\sigma) M_1 = \left(\begin{array}{c|c} h_1^\top \sigma & \\ \vdots & \\ h_n^\top \sigma & 0 \end{array} \right).$$

The spectral norm of this 1-rank matrix is $\sum_i (h_i^\top \sigma)^2$. We proved that Eq. (15) is equivalent to the following optimization problem

$$\begin{aligned} & \underset{\sigma}{\text{maximize}} && \|M_2 \text{diag}(\sigma) M_1\|_2^2 \\ & \text{s. t.} && \sigma \in [0, 1]^n. \end{aligned} \quad (16)$$

We recover the exact formulation of Section 6 Eq. (9) for a 2-layer MLP (the reader can verify there is no recursive loop). Because H is full rank, M_1 is surjective and all σ are admissible values for $g'_i(x)$ which is the equality case. Finally, ReLU activation units take their derivative within $\{0, 1\}$ and Eq. (16) is its relaxed optimization problem, that has the same optimum points.

B Proof of Theorem 3

Consider a single factor $\left\| \tilde{\Sigma} V \text{diag}(\sigma) U^\top \tilde{\Sigma}' \right\|_2$ with V and U unitary matrices and $\tilde{\Sigma}$ (resp. $\tilde{\Sigma}'$) is diagonal with eigenvalues $(s_k)_k$ (resp. $(s'_j)_j$) in decreasing order along the diagonal. Decompose the eigenvalue matrices as $\tilde{\Sigma} = s_1 E_{11} + D$ and $\tilde{\Sigma}' = s'_1 E'_{11} + D'$, by orthogonality we can write

$$\left\| \tilde{\Sigma} V \text{diag}(\sigma) U^\top \tilde{\Sigma}' \right\|_2^2 \leq \left\| s_1 E_{11} V \text{diag}(\sigma) U^\top E'_{11} s'_1 \right. \quad (17)$$

$$\begin{aligned} & + s_1 E_{11} V_i \text{diag}(\sigma) U^\top D' \\ & + D V \text{diag}(\sigma) U^\top E'_{11} s'_1 \Big\|_2^2 \\ & + \|D V \text{diag}(\sigma) U^\top D'\|_2^2. \end{aligned} \quad (18)$$

First we can bound $(4) \leq (s_2 s'_2)^2$. For (3) denote v_k (resp. u_k) the k -th column of V (resp. of U). It follows that

$$(3) \leq (s_1 s'_1)^2 \langle v_1, \sigma \cdot u_1 \rangle^2 + \sum_{j>1} (s_1 s'_j)^2 \langle v_1, \sigma \cdot u_j \rangle^2 + \sum_{k>1} (s_k s'_1)^2 \langle v_k, \sigma \cdot u_1 \rangle^2.$$

The columns $(v_k)_k$ of V form an orthonormal basis so we have

$$\sum_{k>1} \langle v_k, \sigma \cdot u_1 \rangle^2 = \|\sigma \cdot u_1\|^2 - \langle v_1, \sigma \cdot u_1 \rangle^2,$$

and we deduce a similar equality for $\sum_{j>1} \langle v_1, \sigma \cdot u_j \rangle^2$. Using $s_k \leq s_2$ for $k > 1$ we finally obtain

$$(3) \leq (s_1 s'_1)^2 (\langle v_1, \sigma \cdot u_1 \rangle^2 (1 - \tilde{r}_1 - \tilde{r}_2) + \tilde{r}_1 + \tilde{r}_2),$$

with $\tilde{r}_1 = (\frac{s_2}{s_1})^2$ and $\tilde{r}_2 = (\frac{s'_2}{s'_1})^2$. In conclusion we proved the following inequality:

$$\left\| \tilde{\Sigma} V \text{diag}(\sigma) U^\top \tilde{\Sigma}' \right\|_2^2 \leq (s_1 s'_1)^2 ((1 - \tilde{r}_1 - \tilde{r}_2) \langle v_1, \sigma \cdot u_1 \rangle^2 + \tilde{r}_1 + \tilde{r}_2 + \tilde{r}_1 \tilde{r}_2).$$

The Lipschitz upper bound given by AutoLip of $\left\| \tilde{\Sigma}_1 V \text{diag}(\sigma) U^\top \tilde{\Sigma}_2 \right\|_2$ is $s_1 s'_1$. For the middle layers, we have $\tilde{\Sigma} = \Sigma^{1/2}$, and the inequality still holds for the first and last layer due to $\tilde{r}_i \leq \frac{s_2}{s_1}$; taking the maximum for σ leads to the theorem.

C Proof of Lemma 2

Let $U, V \sim \mathcal{N}(0, I_n)$ be two independent n -dimensional Gaussian random vectors. Then, $u = U/\|U\|_2$ and $v = V/\|V\|_2$ are uniform on the unit sphere \mathcal{S}^{n-1} , and

$$\begin{aligned} \max_{\sigma \in [0,1]^n} |\langle \sigma \cdot u, v \rangle| &= \max_{\sigma \in [0,1]^n} \left| \sum_{i=1}^n \sigma_i u_i v_i \right| \\ &= \max \left\{ \sum_{i=1}^n (u_i v_i)^+, \sum_{i=1}^n (u_i v_i)^- \right\}, \end{aligned} \tag{19}$$

where $x^+ = \max\{0, x\}$ and $x^- = \max\{0, -x\}$ are respectively the positive and negative parts of x . Note that $\sum_{i=1}^n (u_i v_i)^+$ and $\sum_{i=1}^n (u_i v_i)^-$ have the same law, since the distribution of u and v is symmetric w.r.t. the coordiante axes. Moreover, we may rewrite

$$\sum_{i=1}^n (u_i v_i)^+ = \frac{\frac{1}{n} \sum_{i=1}^n (U_i V_i)^+}{\sqrt{\frac{1}{n} \sum_{i=1}^n U_i^2} \sqrt{\frac{1}{n} \sum_{i=1}^n V_i^2}}, \tag{20}$$

and each term converges almost surely to its expectation due to the strong law of large numbers. Finally, noting that $\mathbb{E}[U_i^2] = \mathbb{E}[V_i^2] = 1$ and

$$\mathbb{E}[(U_i V_i)^+] = \frac{1}{2} \mathbb{E}[|U_i V_i|] = \frac{1}{2} \mathbb{E}[|U_i|] \mathbb{E}[|V_i|] = \frac{1}{\pi}, \tag{21}$$

leads to the desired result.

D Convolutional Neural Network of Section 7

Each convolution except the last one is followed by a ReLU activation unit.

Layer	# channels out	kernel	stride
Conv2D + bias	32	(5, 5)	2
Conv2D + bias	64	(3, 3)	2
Conv2D + bias	128	(3, 3)	2
Conv2D + bias	10	(2, 2)	1